Influence of Au catalyst on the growth of ZnS nanowires

Ming Lin [a,b], Tripathy Sudhiranjan [b], Chris Boothroyd [b], Kian Ping Loh [a,*]

[a] *Department of Chemistry, National University of Singapore, 3 Science Drive 3, Singapore 117543, Singapore*
[b] *Institute of Material Research and Engineering, 3 Research Link, Singapore*

Abstract

We have successfully prepared dense and uniform ZnS nanowires with hexagonal wurzite structure on Au-coated Si substrate. The growth of the single crystalline ZnS nanowire follows the well-known vapor liquid solid (VLS) mechanism. The initial stages of the nucleation and growth processes of ZnS nano-particles on gold particles have been studied by atomic force microscopy (AFM) to derive insights into the critical nuclei size that promoted the growth of the nanowire. AFM images clearly show the three stages of the VLS growth process. Micro-Raman scattering detects various peaks related to the nanosize effects of the ZnS nanowires.
© 2004 Elsevier B.V. All rights reserved.

1. Introduction

Nanomaterials provide good learning ground for studying the quantum confinement effects and thermodynamic properties specific to the dimensional structures of these materials, which are expected to be different compared to the bulk phase. In a nanotube or nanowire, the finite size effect gives rise to a shift of the zone boundary in the phonon dispersion. Therefore, zone boundary phonons and activated defects due to lattice disorder can manifest in nanoparticles. Micro-Raman technique is a powerful tool for the study of such nano-related effects in nanomaterials. In the case of nanomaterials, quantum size effects come into play besides the enhancement of the surface-to-volume ratio. In addition, resonant Raman effect could give rise to new features in the Raman spectrum of nanomaterials due to resonantly excited zone boundary and disorder-activated modes, which are forbidden in the bulk material [1–3].

ZnS nanowire, a direct bandgap ($E_g \approx 3.7$ eV) inorganic material with wide-ranging technological applications, can be synthesized using Au as the catalysts by simple thermal evaporation of ZnS powder [4,5]. The well-known vapor–liquid–solid (VLS) mechanism [6] can be invoked to explain the growth mechanism of ZnS nanowires. In the VLS process, the liquid metal particles act as catalytic sites for absorption of gas-phase reactants. One dimensional (1D) nanostructures ensue from the supersaturated metal catalyst by precipitation. The size of the growing structure is restricted naturally by the size of the catalyst where it recrystallizes from. However, there are few direct observations of nanowire growth by VLS process. Recently, Yang et al. [7,8] reported direct observation of Ge nanowires and GaN nanowires growth by VLS process using in-situ TEM. Besides TEM, atomic force microscope (AFM) can also be employed to observe the growth of nanomaterials at the initial stages.

In this work, AFM was applied to investigate the initial stages of the nucleation and growth processes of ZnS nanoparticles on Au. Such measurements allow us to probe the critical nuclei size that promotes the growth ZnS nanowires. Micro-Raman technique was also employed to study these nanowires in order to see if nano-related features not observable in the bulk-phase can be detected.

---

* Corresponding author. Fax: +65 6779 1691.
  E-mail address: chmlohkp@nus.edu.sg (K.P. Loh).

2. Experimental

ZnS nanowires were grown by thermally evaporating commercial ZnS powder onto the gold-coated silicon substrate, with the substrate temperature maintained at 700 °C under a dynamic vacuum of 1×10^{-5} torr. The powder was evaporated using high temperature Knudsen cell operated at different temperatures, with the growth time limited to 1 min. Before the cell reached the required temperature, the shutter was closed and the substrate was kept remote from the ZnS source to prevent deposition. Structural and morphological characterization of the ZnS films was carried out using SEM (Joel-JSM 6700F), high-resolution TEM (Phillips CM300), and AFM. Micro-Raman measurements were carried out using 514.5 nm line excitation from an Ar^+ laser at room temperature. The scattered light was dispersed through a JYT64000 set up equipped with liquid nitrogen cooled CCD.

3. Results and discussion

Fig. 1 shows the SEM micrograph of the ZnS film prepared on silicon. Bulk quantities of densely packed nanowires, with an average diameter of about 80–100 nm and length of 10 μm, can be grown. Energy dispersive X-ray spectroscopy (EDX) shows that these nanowires are composed mainly of Zn and S. Grazing angle X-ray diffraction (XRD) confirms that all the reflected peaks with preferred orientation (0 0 2) can be indexed to ZnS hexagonal wurtzite structure with lattice constants $a = 3.80$ and $c = 6.23$ Å. TEM image of the ZnS nanowire and select area diffraction pattern taken from the (0 0 2) plane is shown in Fig. 2. The image shows that these ZnS nanowires are uniform
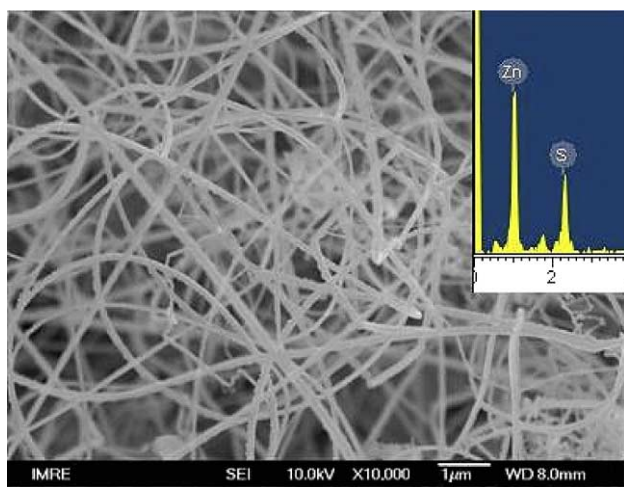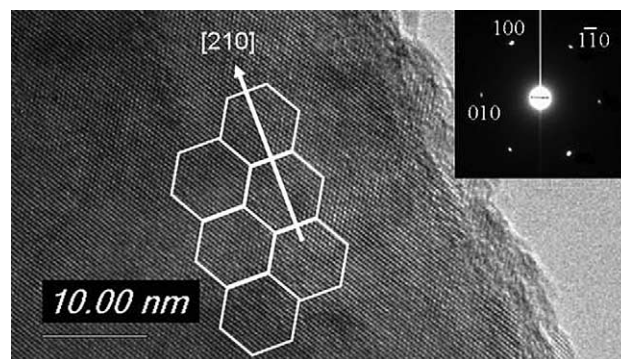

Fig. 2. High-resolution TEM image of ZnS nanowire. Inset shows the selected area diffraction pattern recorded at the same area.

and single crystalline. The resolved lattice spacing is approximately 0.32 nm between adjacent crystal planes, which corresponds to the distance between (1 0 0) planes, confirming that [2 1 0] is the growth direction.

To characterize the structural evolution of these ZnS nanowires during the various growth stages, AFM measurements were carried out. Fig. 3 shows the sequences of AFM images captured during different ZnS growth stages. Three distinct stages can be observed:

(i) *Aggregation.* The thickness of the Au film deposited by e-beam deposition is around 10 nm. Fig. 3a shows uniform and smooth Au film on Si substrate before annealing. After 700 °C annealing, the Au film aggregates to form small islands with an average diameter of 200 nm (Fig. 3b). This is due to the liquid-like mobility of Au atoms at high temperature.

(ii) *Alloying and nucleation.* Fig. 3c shows the morphology of the film exposed to ZnS vapor, which was precisely controlled by evaporating ZnS powder at 870 °C for 1 min. From AFM image, these particles are two times larger than those of pure Au islands, suggesting that ZnS and Au form an alloy with increased volume.

(iii) *Saturation and growth.* With an increase of the evaporation temperature of ZnS powder to 920 °C, ZnS nanowires are observed to grow from the Au/ZnS alloys (one min growth) in Fig. 3d. The use of higher vapor pressure readily supersaturates the molten Au with ZnS, and subsequent recrystallization of ZnS nanowire from the saturated melt occurs.

Since (1 0 0) face is one of the most stable faces in ZnS crystal with the lowest surface energy, most of these nanowires would grow along [2 1 0] direction normal to the (1 0 0) planes. The substrate temperature determines the saturation ratio of ZnS and two competitive growth
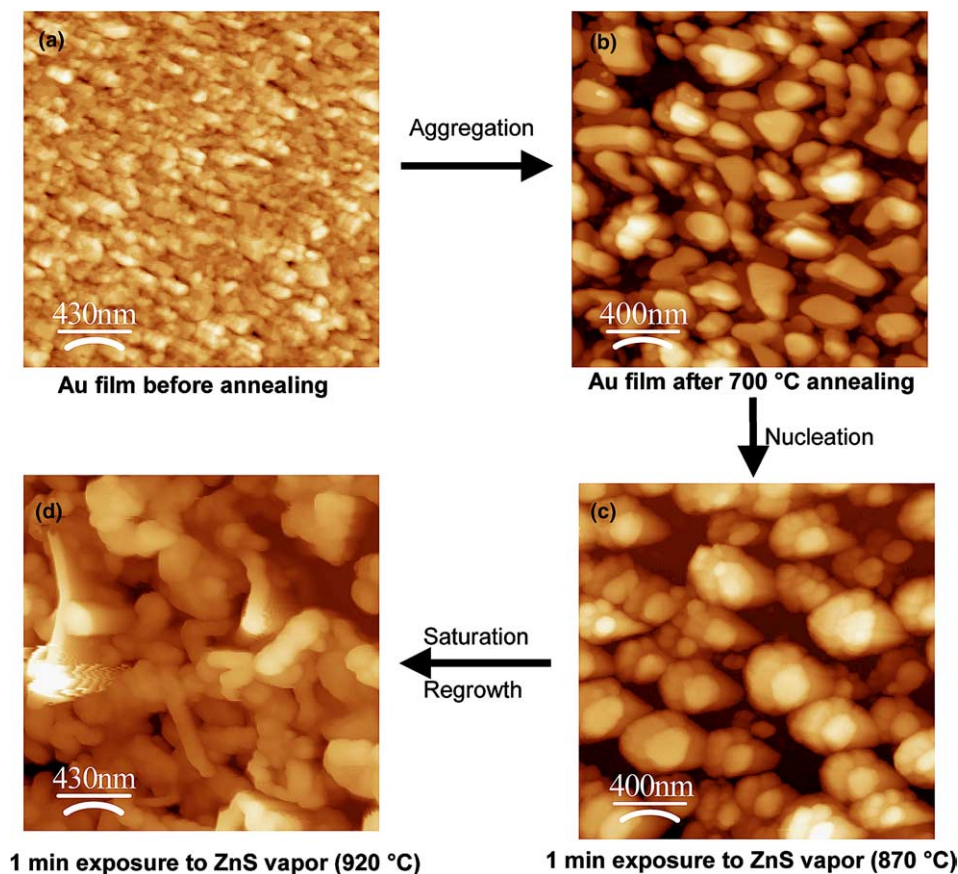

Fig. 1. SEM image of ZnS nanowires grown on Si. The inset shows a localized EDX spectrum of a ZnS nanowire.

Fig. 3. AFM images of the different stages during the growth of ZnS nanowire.

directions. Higher temperature (>900 °C) prompts the growth along [1 1 0] direction [5], while relatively lower temperature around 700–800 °C benefits the growth along the [2 1 0] direction.

Raman spectra obtained from the ZnS nanowires and commercial ZnS powders are shown in Fig. 4. The much weaker peak at 520.7 cm^{-1} arises from Si substrate. Compared to the spectrum of the ZnS powder, the spectrum of ZnS nanowires is dominated by the longitudinal optical (LO) phonon peak of ZnS at 348.5 cm^{-1}. The weaker peak near 266.5 cm^{-1} is associated with the transverse optical (TO) phonon. Since most of these nanowires were grown along one direction, certain phonon peaks allowed by the selection rules will become stronger in a particular scattering geometry. When the propagation is along one direction, the polar phonon will be purely longitudinal due to Raman selection rules. Compared to the Raman spectrum of bulk hexagonal ZnS (TO: 274 cm^{-1} and LO: 352 cm^{-1}), the peaks of the first-order LO and TO phonons from these ZnS nanowires exhibit a shift towards the lower energy. In addition, the Raman line showed substantial broadening. Such phonon softening and line broadening of the Raman peaks can be associated with quantum confinement effects. The relaxation of the wave-vector selection rule in these nanocrystals and the size dispersion of the

nanowires resulted in the shift, as well as the broadening of the TO and LO peaks.

Apart from these characteristics peaks, Raman peaks near 155, 178, 217.5, 418.5, 442.5 and 667.5 cm^{-1} are also observed. The appearance of these phonon features
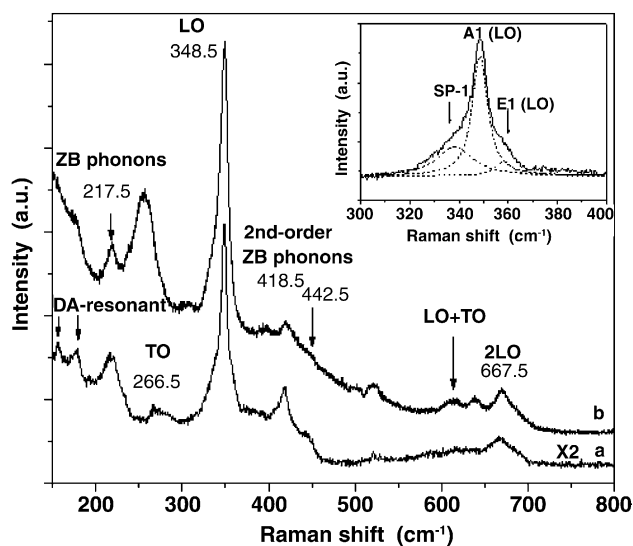

Fig. 4. Raman spectrum of ZnS: (a) nanowires, (b) powders. The inset shows spectral deconvolution of the LO phonon of the ZnS nanowires.

from ZnS nanowires could be due to plasmon-enhanced resonant Raman effect [9,10]. The presence of gold catalyst could be responsible for the selective enhancement of Raman intensity by plasmon scattering at the ZnS/Au interface. Such effects could give rise to the observation of disorder-activated (DA) modes. This is evident from the peaks at 155 and 178 cm^{-1}, which are assigned as disorder activated second order acoustic phonons. These peaks could only be observed from 8 nm ZnS nanoparticles in control studies [9,10]. The possibility of observing these features from our much larger ZnS nanowires may be due to surface enhancement effect promoted by the gold particles. In addition, formation of such nanowires leads to a breakdown of the $\vec{q} = 0$ Raman selection rule in the Brillouin zone. As a result, the zone boundary phonons, their first and second-order combination modes and intermediate q values phonons become active. For example, the modes near 217.5, 418.5, and 442.5 cm^{-1} are due to the first order and second order zone-boundary (ZB) phonons. A much weaker and broader band near 667.5 cm^{-1} can be associated with the second order LO phonon.

The increased surface-to-volume ratio of nanowires will result in a stronger surface phonon peak relative to the bulk phonon peak. As a result, the intensity of the surface phonon peak becomes stronger in these ZnS nanowires. Taking into account the cylindrical symmetry for the shape of these ZnS nanowires, the surface phonon w_s can be theoretically calculated using the following equation [11,12]:

$$w_s[\varepsilon_\infty(1 + \varepsilon_0)/\varepsilon_0(1 + \varepsilon_\infty)]w_{LO}, \tag{1}$$

where ε_0 (=8.50) and ε_∞ (=5.10) [13] are the static and high frequency dielectric constants and w_{LO} is the longitudinal optical frequency measured in this spectrum. The calculated surface phonon frequency of LO peak is 337 cm^{-1}. The inset in Fig. 4 shows a multiple Lorentzian peak fitting around the LO-phonon. The peak near 338.4 cm^{-1} can be associated with a surface phonon, which is in good agreement with the calculated frequency of the surface mode. The presence of the high-energy shoulder at 355 cm^{-1} around the LO phonon is due to a splitting of the LO phonon into $A_1(LO)$ and $E_1(LO)$ component arising from the surface polarization effects in ZnS nanowires.

In conclusion, we have successfully grown ZnS nanowires with the hexagonal wurtzite structure. The three stages of the VLS growth process have been documented in a sequential fashion using AFM. Apart from characteristics LO phonons, micro-Raman scattering detects various nano-related peaks unique to the ZnS nanowire.

Acknowledgements

References

[1] F.J. Brieler, P. Grundmann, M. Froba, L.M. Chen, P.J. Klar, W. Heimbrodt, H.A.K. von Nidda, T. Kurz, A. Loidl, J. Am. Chem. Soc. 126 (2004) 797.
[2] A.V. Baranov, Y.P. Rakovich, J.F. Donegan, T.S. Perova, R.A. Moore, D.V. Talapin, A.L. Rogach, Y. Masumoto, I. Nabiev, Phys. Rev. B 68 (2003) 165036.
[3] R.D. Yang, S. Tripathy, F.E.H. Tay, L.M. Gan, S.J. Chua, J. Vac. Sci. Technol. B 21 (2003) 984.
[4] X.M. Meng, J. Liu, Y. Jiang, W.W. Chen, C.S. Lee, I. Bello, S.T. Lee, Chem. Phys. Lett. 382 (2003) 434.
[5] Y.W. Wang, L.D. Zhang, C.H. Liang, G.Z. Wang, X.S. Peng, Chem. Phys. Lett. 357 (2002) 314.
[6] E.I. GivargizovModern Crystallography, vol. III, Springer, Berlin, 1984.
[7] E.A. Stach, P.J. Pauzauskie, T. Kuykendall, J. Goldberger, R.R. He, P.D. Yang, Nano Lett. 3 (2003) 867.
[8] Y.Y. Wu, P.D. Yang, J. Am. Chem. Soc. 123 (2001) 3165.
[9] M. Abdulkhadar, B. thomas, Nanostruc. Mater. 5 (1995) 289.
[10] S.M. Scholz, R. Vacassy, L. Lemaire, J. Dutta, H. Hofmann, Appl. Organomet. Chem. 12 (1998) 327.
[11] J.F. Scott, T.C. Damen, Opt. Commun. 5 (1972) 410.
[12] P. Clippe, R. Evrard, A.A. Lucas, Phy. Rev. B 14 (1976) 1715.
[13] T. Yamamoto, Jpn. J. Appl. Phys. 42 (2003) L514.